

A Five-Coordinate Carbon Center and Zr to H, B, and C Bonding in $\text{Cp}_2\text{Zr}[\text{CH}_2(\text{BH}\{\text{C}_6\text{F}_5\}_2)_2]$

Udo Radius,[†] Sandro Johannes Silverio,[‡] Roald Hoffmann,^{*,†} and Rolf Gleiter^{*,‡}

Department of Chemistry, Baker Laboratory, Cornell University, Ithaca, New York 14853-1301, and Organisch-Chemisches Institut der Universität Heidelberg, Im Neuenheimer Feld 270, 69120 Heidelberg, Germany

Received February 12, 1996[®]

The electronic structure of $\text{Cp}_2\text{Zr}[\text{CH}_2(\text{BH}\{\text{C}_6\text{F}_5\}_2)_2]$, an intriguing compound recently synthesized by Piers and co-workers, is analyzed by means of molecular orbital calculations. The methods applied were of the extended Hückel type, as well as *ab initio* calculations at the RHF and RMP2 levels, and density functional theory (DFT). This mononuclear complex is of interest due to the exceptional, 5-fold coordination of its methylene carbon atom, which assumes a distorted near trigonal-bipyramidal geometry with definite Zr–C bonding. The factors stabilizing half-planar methane, the simplest organic molecule resembling the conformation of the carbon atom found in the complex under study, as well as the electronic structure of the compound are discussed. Half-planar methane may be stabilized by σ -donor (and/or π -acceptor) ligands in the axial plane and by an external, coordinating σ -acceptor in the equatorial plane. Both features are found in the Piers compound. In this molecule the ligand is ideally oriented for making use of the bonding potential of the two a_1 and one b_2 MOs of the Cp_2Zr fragment. There is Zr–H(B), Zr–B, and Zr–C bonding in this molecule.

Introduction

In 1970, it was suggested that the seemingly impossible goal of stabilizing a planar tetracoordinate carbon might not be out of reach.¹ A planar conformation for a methane-like molecule implies weakened electron-deficient three-center σ -bonding between carbon and the four ligands bound to it, while the carbon's two remaining valence electrons occupy an undisturbed, high-lying carbon 2p π -orbital. For methane itself, this planar conformation is destabilized by a considerable amount of energy, probably more than the C–H bond strength.

The theoretical strategy suggested to reduce the gigantic barrier to planarization was based on the replacement of the four hydrogen atoms by substituents that are (i) σ -donors, to facilitate electron transfer to the electron deficient carbon, and (ii) π -acceptors, to delocalize the p- or π -type lone pair. These proposals were substantiated and extended by Schleyer et al.,² who carried out Hartree–Fock self-consistent field calculations on several model species with ligand atoms or groups containing Li, B, and Si and also with the carbon atom incorporated in small rings. Since that time there have been many other theoretical studies and some experimental approaches to square planar carbon.³

The last few years have brought us a number of organometallic compounds with the exceptional “anti van't Hoff/Le Bel” arrangement for the carbon atom, i.e. molecules with stabilized planar tetracoordinated carbon. The first of those compounds— $\text{V}_2(\text{DMP})_4$ (DMP =

dimethoxyphenyl)—was synthesized by Seidel and co-workers in 1976^{4a} and structurally characterized 1 year later by Cotton and Millar.^{4b} Quantum chemical analysis of its electronic structure showed that the planar tetracoordinate carbon atom is stabilized through donation of the carbon lone pair toward fragment orbitals delocalized on the two metal atoms.^{4c} Recent experimental work in Erker's group⁵ on quite different binuclear $[\text{Zr}]$ – $[\text{M}]$ complexes ($[\text{M}] = \text{B}, \text{Al}, \text{Ga}, \text{Zr}$) has revived interest in these unusual carbon configurations. Gleiter et al.⁶ interpreted the stabilization of the planar tetracoordinate carbon in Erker's complexes by the presence of a σ -acceptor substituent d^0 - $[\text{Cp}_2\text{Zr}]^{2+}$.

The process of planarizing methane can be viewed either as “squashing” (opening up two opposite angles while retaining D_{2d} symmetry) or “twisting” (one CR_2

(3) (a) Hoffmann, R. *Acc. Chem. Res.* **1971**, *4*, 1. (b) Minkin, V. I.; Minyaev, R. M.; Zhadov, Y. A. *Nonclassical structures of Organic Compounds*; MIR Publishers: Moscow, 1987. (c) Sorger, K.; Schleyer, P. v. R.; *Theochem* **1995**, *338*, 317. (d) Dodziuk, H.; Leszczyński, J.; Nowiński, K. S. *J. Org. Chem.* **1995**, *60*, 6860 and references cited therein.

(4) (a) Seidel, W.; Kreisel, G.; Mennenga, H. *Z. Chem.* **1976**, *16*, 492. (b) Cotton, F. A.; Millar, M. *J. Am. Chem. Soc.* **1977**, *99*, 7886. (c) Poubmga, C. N.; Bénard, M.; Hyla-Kryspin, I. *J. Am. Chem. Soc.* **1994**, *116*, 8259.

(5) (a) Erker, G.; Zwettler, R.; Krüger, C.; Noe, R.; Werner, S. *J. Am. Chem. Soc.* **1990**, *112*, 9620. (b) Erker, G.; Albrecht, M.; Werner, S.; Nolte, M.; Krüger, C. *Chem. Ber.* **1992**, *125*, 1953. (c) Erker, G.; Albrecht, M.; Krüger, C.; Werner, S.; Binger, P.; Langhauser, F. *Organometallics* **1992**, *11*, 3517. (d) Erker, G.; Albrecht, M.; Krüger, C.; Werner, S. *J. Am. Chem. Soc.* **1992**, *114*, 8531. (e) Erker, G. *Comments Inorg. Chem.* **1992**, *13*, 111. (f) Erker, G. *Nachr. Chem. Techn. Lab.* **1992**, *40*, 1099. (g) Albrecht, M.; Erker, G.; Krüger, C. *Synlett* **1993**, 441. (h) Erker, G.; Albrecht, M.; Krüger, C.; Nolte, M.; Werner, S. *Organometallics* **1993**, *12*, 4979. (i) Binger, P.; Sandmeyer, F.; Krüger, C.; Kuhnigk, J.; Goddard, R.; Erker, G. *Angew. Chem.* **1994**, *106*, 213; *Angew. Chem., Int. Ed. Engl.* **1994**, *33*, 197. (j) Binger, P.; Sandmeyer, F.; Krüger, C.; Erker, G. *Tetrahedron* **1995**, *51*, 4277.

(6) (a) Gleiter, R.; Hyla-Kryspin, I.; Niu, S.; Erker, G. *Angew. Chem.* **1993**, *105*, 753; *Angew. Chem., Int. Ed. Engl.* **1993**, *32*, 754. (b) Gleiter, R.; Silverio, S. J.; Binger, F.; Sandmeyer, P.; Erker, G. *Chem. Ber.* **1995**, *128*, 775. (c) Röttger, D.; Erker, G.; Fröhlich, R.; Grehl, M.; Silverio, S. J.; Hyla-Kryspin, I.; Gleiter, R. *J. Am. Chem. Soc.* **1995**, *117*, 10503.

[†] Cornell University.

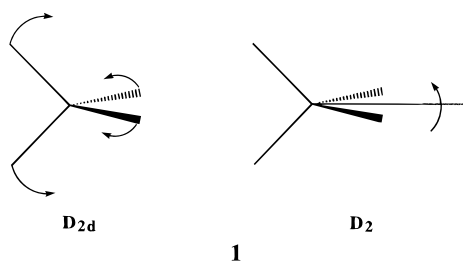
[‡] Organisch-Chemisches Institut der Universität Heidelberg.

[®] Abstract published in *Advance ACS Abstracts*, August 1, 1996.

(1) Hoffmann, R.; Alder, R. W.; Wilcox, C. F. *J. Am. Chem. Soc.* **1970**, *92*, 4992.

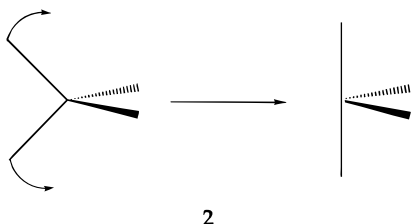
(2) Collins, J. B.; Hill, J. D.; Jemmins, E. D.; Apeloig, Y.; Schleyer, P. v. R.; Seeger, R.; Pople, D. A. *J. Am. Chem. Soc.* **1976**, *98*, 5419.

angle twisted vs the opposing one, D_2), **1**.



Actually these motions are not as distinct as they seem.⁷ Each involves a great increase in some R–C–R angle; this is a much more difficult thing to achieve (through molecular architectural constraints) than closing such an angle down.

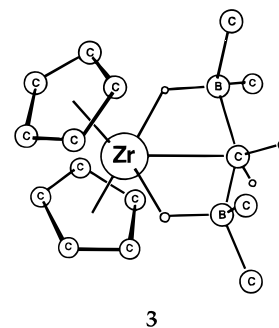
There is another deformation of tetrahedral carbon, which can be seen as related to the planarization discussed above, and this is the “half-planarization”, illustrated in **2**. The resulting geometry is obviously related to a trigonal bipyramid minus one ligand or to the SF₄ structure.



There are some examples of derivatives of half-planar carbon stabilized in organometallic complexes.⁸ In these compounds one effectively has five-coordinate methylene carbon atoms with a distorted trigonal-bipyramidal coordination geometry. The examples known are generally “ate” complexes, negatively charged compounds with lithium counterions in the carbon ligand sphere, such as Evans’ (Me₃SiCH₂)Y[(μ-CH₂)₂SiMe₂][(μ-OtBu)-Li(THF)₂]₂^{8a} or a similar samarium compound made by Clark et al.^{8b} Five-coordinate carbon atoms have been observed previously but generally with a methylene carbon or alkyl group bridging a binuclear metal center in a three-center, two-electron bonding mode.^{9,10} There is also a lore of trying to stabilize the five-coordinate trigonal bipyramidal carbon which is the transition state of an S_N2 reaction.¹¹

Most recently, Piers et al.,¹² in the course of their investigation on the reactivity of the electrophilic borane HB(C₆F₅)₂ toward alkylzirconium complexes, published the synthesis and structure of Cp₂Zr[CH₂(HB{C₆F₅})₂],

3 (only the C_{ipso} carbon atoms of the perfluorinated phenyl groups are shown).



This complex appears to be the first mononuclear organometallic compound stabilizing a pentacoordinate carbon atom, which is not an “ate” complex. A X-ray analysis of **3** as a benzene solvate¹² reveals the unique bonding arrangement, in which the methylene carbon is approximately trigonal-bipyramidally coordinated. The environment of the carbon contains two hydrogen atoms and the metal of the bent metallocene unit in what we will call the equatorial plane and two axial-substituted borane groups HB(C₆F₅)₂. The zirconium–carbon distance is 2.419(4) Å, 0.046 Å longer than the bond length of the central zirconium atom to the C_{inside} atom of the ethylene ligand in Cp₂Zr(PMe₃)(η²-C₂H₄).¹³ We think this distance is definitely to be regarded as a bonding contact, and we will support that contention below.

The B–C–B angle of 149.3(4)° is highly unusual, significantly larger than expected values. The sum of the angles spanned by the three ligands in the equatorial plane of the methylene carbon atom is 358°, but the atoms are not in an ideal trigonal arrangement. The CH₂ unit appears to be tilted, resulting in Zr–C–H angles of 107 and 149°, respectively. We note here the usual reservations one must have about the position of hydrogen atoms located in X-ray crystallographic structure determinations.

The Model and Computational Details

The model compounds we used in our calculations were **4**, **5**, **6** and **4'**, **5'**, **6'**, **6''**.

We replaced the four C₆F₅ ligands attached to boron in the case of the simplest model compound **4** by four hydrogen groups and symmetrized the molecule to a C_{2v} structure with a planar six membered heterocyclic ring {–Zr–H–B–C–B–H–}. In **5** the substituents are methyl groups, and in **6** we substituted the C₆F₅ ligands by F atoms (to mimic the π-donor and σ-acceptor properties of a C₆F₅ ring). The distances available from the X-ray structure determination were averaged and used in our calculations, with the exception of the

(7) (a) Lohr, L. L. *J. Am. Chem. Soc.* **1978**, *100*, 1093. (b) Halevi, E. A.; Knorr, R. *Angew. Chem.* **1982**, *94*, 307; *Angew. Chem., Int. Ed. Engl.* **1982**, *21*, 288.

(8) (a) Evans, W. J.; Boyle, T. J.; Ziller, J. W. *J. Organomet. Chem.* **1993**, *462*, 141. (b) Clark, D. L.; Gordon, J. C.; Huffman, J. C.; Watkin, J. G.; Zwick, B. D.; *Organometallics* **1994**, *13*, 4266.

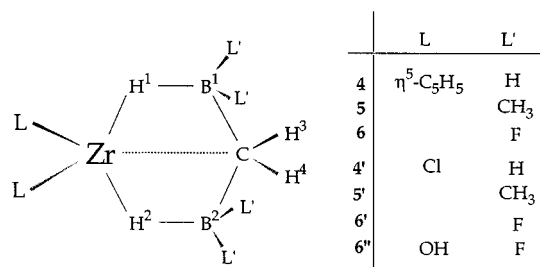
(9) Holton, J.; Lappert, M. F.; Pearce, R.; Yarrow, P. I. W. *Chem. Rev.* **1983**, *83*, 135.

(10) (a) Morris, R. J.; Girolami, G. S. *Organometallics* **1989**, *8*, 1478. (b) Jarvis, J. A.; Pearce, R.; Lappert, M. F.; *J. Chem. Soc., Dalton Trans.* **1977**, 999. (c) Hursthouse, M. B.; Malik, K. M. A.; Sales, K. D. *J. Chem. Soc., Dalton Trans.* **1978**, 1314. (d) Davies, J. I.; Howard, C. G.; Skapski, A. C.; Wilkinson, G. *J. Chem. Soc., Chem. Commun.* **1982**, 1077. (e) Howard, C. G.; Wilkinson, G.; Thornton-Pett, M.; Hursthouse, M. B. *J. Chem. Soc., Dalton Trans.* **1983**, 2025.

(11) (a) Gleiter, R.; Hoffmann, R. *Tetrahedron* **1968**, *24*, 5899. (b) Cifffarin, E.; Fava, A. *Prog. Phys. Org. Chem.* **1968**, *6*, 81. (c) Jencks, W. P. *Chem. Rev.* **1981**, *10*, 345. (d) Shaik, S. S. *Prog. Phys. Org. Chem.* **1985**, *15*, 197. (e) Minkin, V. I.; Simkin, B. Ya.; Minyaey, R. M. *Quantum Chemistry of Organic Compounds—Mechanisms of Reactions*; Springer: Heidelberg, Germany, **1990**; Chapter 5.1. (f) Shaik, S. S.; Schlegel, H. B.; Wolfe, S. *Theoretical Aspects of Physical Organic Chemistry—The S_N2 Mechanism*; Wiley: New York, 1992. (g) Rauk, A. *Orbital Interaction Theory of Organic Chemistry*; Wiley: New York, 1994; Chapter 9.

(12) Spence, R. E. v. H.; Parks, D. J.; Piers, W. E.; MacDonald, M.-A.; Zaworotko, M. J.; Rettig, S. J. *Angew. Chem.* **1995**, *107*, 1337; *Angew. Chem., Int. Ed. Engl.* **1995**, *34*, 1230.

(13) Alt, H. G.; Denner, C. E.; Thewalt, U.; Rausch, M. D. *J. Organomet. Chem.* **1988**, *356*, C83.



published carbon–hydrogen bond lengths, which were adjusted to a more realistic 1.10 Å. The distances and angles used are listed in the Appendix. In **4'**, **5'**, and **6'** we use Cl as a replacement for the Cp rings and OH in the case of **6''**. Recent studies have shown that such substitutions reduce computer time but do not affect the essential electronic features of the system.^{6,14}

We have carried out molecular orbital (MO) calculations of quite different types in order to get some insight into the bonding of complex **3**, particularly to discern the electronic features that stabilize the 5-fold coordination geometry at the carbon atom. Single point calculations were carried out on model compounds **4**, **5**, and **6** applying the extended Hückel (EH) and *ab initio* restricted Hartree–Fock (RHF) procedures. Details of the EH calculation are provided in the Appendix. MP2 (Møller–Plesset perturbation theory terminated at second order)¹⁵ and DFT (density-functional theory) methods were also used (with geometry optimization under a C_s symmetry constraint) for model compounds **5'**, **6'**, and **6''**. We have taken in our DFT calculations Becke's three parameter hybrid method¹⁶ using the correlation functional of Lee, Yang, and Parr,¹⁷ which includes both local and nonlocal terms. The symmetry was lowered to C_1 in the case of **6'** and **6''** so as to investigate the skewing of the methylene group suggested by the crystal structure determination. Relativistic pseudopotentials were employed for inner shell electrons of Zr and Cl as suggested by Hay and Wadt.¹⁸ The valence orbitals, and in the case of Zr also the outermost core orbitals, are treated as a Gaussian orbital basis set (4s, 4p, 4d, 5s, 5p) for Zr and (3s, 3p) in the case of Cl. The valence orbitals are contracted to a double- ξ basis.

A split-valence basis for C(10s, 5p), B(10s, 5p), F(10s, 5p), O(10s, 5p), and H(4s) was used, as suggested by Dunning and Hay.¹⁹ We used the Gaussian 94 program²⁰ for our *ab initio* and DFT calculations.

Extended Hückel Investigation of Half-Planar Methane

The C_{2v} structure of half-planar methane can be related to either a square-planar or a tetrahedral geometry. Both extremes serve as good starting points

(14) (a) Koga, N.; Morokuma, K.; *Chem. Rev.* **1991**, *91*, 823 and references cited therein. (b) Kawamura-Kuribayashi, H.; Koga, N.; Morokuma, K.; *J. Am. Chem. Soc.* **1992**, *114*, 2359. (c) Castonguay, L. A.; Rappé, A. K.; *J. Am. Chem. Soc.* **1992**, *114*, 5832.

(15) (a) Møller, C.; Plesset, M. S.; *Phys. Rev.* **1934**, *46*, 618. (b) Binkley, J. S.; Pople, J. A.; *Int. J. Quantum Chem.* **1975**, *9*, 229.

(16) Becke, A. D.; *J. Chem. Phys.* **1993**, *98*, 5648.

(17) Lee, C.; Yang, W.; Parr, R. G.; *Phys. Rev.* **1988**, *B37*, 785.

(18) (a) Hay, P. J.; Wadt, W. R.; *J. Chem. Phys.* **1985**, *82*, 270. (b) Hay, P. J.; Wadt, W. R.; *J. Chem. Phys.* **1985**, *82*, 284. (18c) Hay, P. J.; Wadt, W. R.; *J. Chem. Phys.* **1985**, *82*, 299.

(19) Dunning, T. H.; Hay, P. J.; *Modern Theoretical Chemistry*; Plenum Press: New York, 1976.

(20) Gaussian 94, Revision B.1: Frisch, M. J.; Trucks, G. W.; Schlegel, H. B.; Gill, P. M. W.; Johnson, B. G.; Robb, M. A.; Cheeseman, J. R.; Keith, T.; Petersson, G. A.; Montgomery, J. A.; Raghavachari, K.; Al-Laham, M. A.; Zakrzewski, V. G.; Ortiz, J. V.; Foresman, J. B.; Cioslowski, J.; Stefanov, B. B.; Nanayakkara, A.; Challacombe, M.; Peng, C. Y.; Ayala, P. Y.; Chen, W.; Wong, M. W.; Andres, J. L.; Replogle, E. S.; Gomperts, R.; Martin, R. L.; Fox, D. J.; Binkley, J. S.; Defrees, D. J.; Baker, J.; Stewart, J. P.; Head-Gordon, M.; Gonzalez, C.; Pople, J. A. Gaussian Inc., Pittsburgh, PA, 1995.

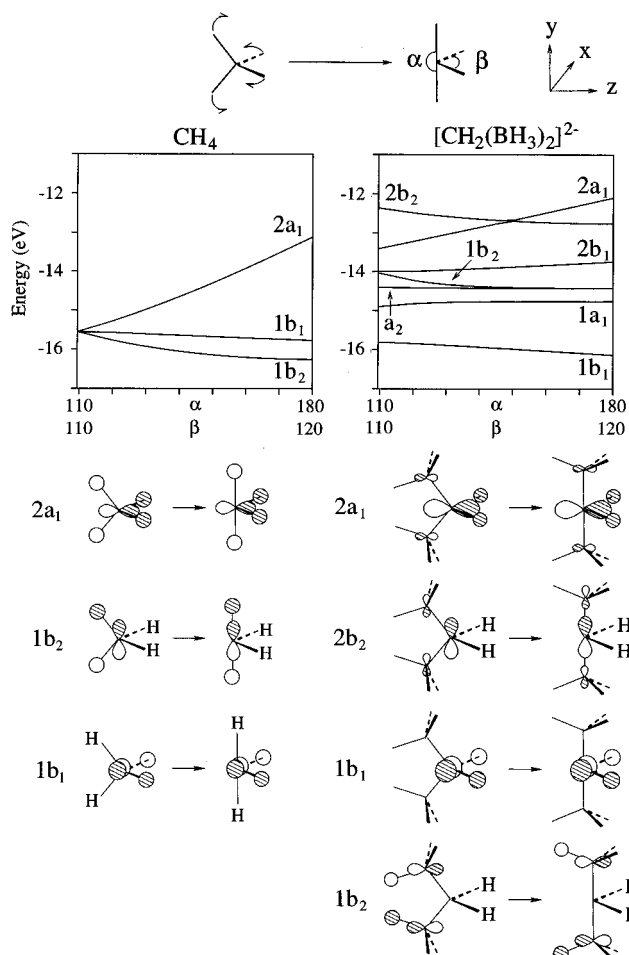


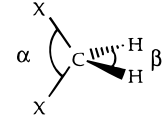
Figure 1. Walsh diagram for a linear transformation of CH_4 (left) and $[CH_2(BH_3)_2]^{2-}$ (right) from a tetrahedral to a half-planar structure. All the orbitals in this figure are occupied.

for this analysis. As a first step, we decided to compare tetrahedral methane and half-planar CH_4 . A Walsh diagram for the transformation of tetrahedral to half-planar CH_4 , depicted in the left part of Figure 1, explains why this deformation is costly in energy.

Shown are the energies of the occupied frontier orbitals (t_2 in T_d) as a function of a linear transit of the angles H–C–H from 109.5 to 180 (α) and 120° (β), respectively, as well as a schematic illustration of these orbitals at the beginning and the end of this transit. The coordinate system is given in the figure—the y axis is that of the linear H–C–H grouping at the half-planar extreme. The z axis is that of the forming “empty coordination site”. Of the three p orbitals on carbon, p_y gains bonding overlap ($1b_2$), whereas p_z rapidly rises in energy ($2a_1$) and becomes directed toward the empty coordination site. If one were to continue to the square planar geometry by opening β to 180°, $2a_1$ would become the pure p_z lone pair of square planar CH_4 . Orbital p_x is almost not affected by a small change of the β angle from 109.5 to 120°. Thus it is the p_z $2a_1$ orbital which is mainly responsible for CH_4 not having a half-planar structure.

The right part of Figure 1 shows the Walsh diagram for the distortion of the dianionic molecule $[CH_2(BH_3)_2]^{2-}$, in the region of –11 to –17 eV. All orbitals in this energy window are occupied. Since there are many orbitals, the picture is more complex than for CH_4 . In

Table 1. Calculated Deformation Energies, Carbon Net Charges, and Carbon Orbital Occupations of CH_2X_2 ($\text{X} = \text{H}, \text{CH}_3, \text{OH}, \text{CN}, \text{BH}_3^-$)



	X				
	H	CH ₃	OH	CN	BH ₃ ⁻
min energy conformer (deg)					
α	109.5	117	112	114	120
β	109.5	105	117	107	102
ΔE_{HP} (eV); ^a α = 180°, β = 120°	3.06	3.76	6.46	2.70	2.06
ΔE_{SB} (eV); ^b α = 150°, β = 104°	0.98	1.15	2.65	0.93	0.54
net charge on C	-0.439	-0.386	0.821	-0.005	-0.958
aop ^c C p _y	0.901	0.857	0.494	0.802	1.190
aop C p _z	1.361	1.397	0.732	1.2297	1.524

^a ΔE_{HP} (eV): deformation energy between the minimum energy structure and the half planar form. ^b ΔE_{SB} (eV): deformation energy between the minimum energy structure and the geometry corresponding to **3**. ^c aop: atomic orbital population.

principle, the same carbon orbitals are affected by the geometrical distortion of CH_4 or $[\text{CH}_2(\text{BH}_3)_2]^{2-}$, namely the orbitals $2a_1$ (C p_z), $1b_2$ or $2b_2$ (C p_y), respectively, and $1b_1$ (C p_x). The difference between CH_4 and the boron-substituted model is mainly due to the $2a_1$ orbital, which is destabilized in the course of the transformation for methane by 2.44 eV and for $[\text{CH}_2(\text{BH}_3)_2]^{2-}$ by 1.38 eV. The differential is less for orbitals $1b_1$ or $1b_2/2b_2$, altogether a stabilization of 0.92 eV for methane compared to 0.76 eV for the boron compound.

Table 1 shows carbon net charges and orbital occupations as well as EH-computed deformation energies to the half planar form (α = 180°, β = 120°), ΔE_{HP} , and to the strongly bent form found in **3** (α = 150°, β = 104°), ΔE_{SB} , of molecules CH_2X_2 with different substituents X (H, CH₃, OH, CN, BH₃⁻). The deformation energies are defined as the difference in energy between the minimum energy conformation and the specified distorted geometry.

We calculate an energy difference of 3.06 eV between the tetrahedral and half-planar structure for methane. The atomic orbital occupation of the p_z orbital increases in the course of the transformation by approximately 0.40 electrons (from 0.962 to 1.361). The overlap population between carbon and the axial hydrogen atoms, not shown in Table 1, drops (from 0.781 to 0.682), as does the atomic orbital occupation of the H_{axial} s and C p_y orbitals. We calculate considerable electron transfer from the axial hydrogen atoms to the carbon atom and a decrease of the C p_y orbital occupation. Thus, half-planar methane should be stabilized by substitution of the axial hydrogen atoms by good σ-donor ligands and/or π-acceptor ligands. This conformation may also be stabilized by the introduction of an external σ acceptor group, a fifth ligand, which could interact with the high lying $2a_1$ (p_z) orbital.

The energy values given in Table 1 support this argument. There is a correlation between the computed carbon net charge (and therefore with the occupation of mainly C p_y and C p_z) and the deformation energies for molecules with σ donor ligands X. Compounds with a more negative carbon net charge in general have a lower deformation energy. The most impressive ex-

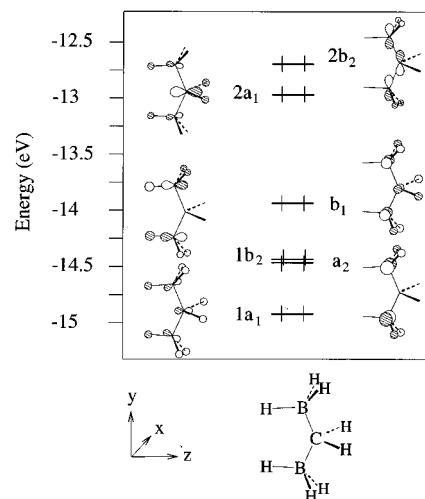


Figure 2. Frontier orbitals of $[\text{CH}_2(\text{BH}_3)_2]^{2-}$.

ample is $\text{CH}_2(\text{OH})_2$, where X is an electronegative group, leading to a positive charge on the carbon atom and relatively small atomic orbital occupations of C p_z and C p_y. The calculated deformation energy, ΔE_{HP} , is 3.40 eV higher than that of methane. Of the first four entries in Table 1, only the molecule with the π-acceptor ligand X = CN reduces ΔE_{HP} relative to methane.

Table 1 also shows the unusual role of BH₃⁻ as a substituent. The substitution of the two axial hydrogen atoms by [BH₃]⁻ groups, excellent σ donors and isolobal to H or CH₃, leads to a decrease of the energy barrier for the deformation to 2.06 eV.

The atomic orbital occupation of the methylene carbon orbitals in $[\text{CH}_2(\text{BH}_3)_2]^{2-}$ in the half-planar geometry is generally higher than for methane with this structure, but most significantly the populations of p_y (1.190 electrons vs 0.901 electrons in half-planar CH₄) and p_z (1.524 vs 1.361 electrons) are increased.

Half-planar methane is stabilized by the introduction of σ-donating [BH₃]⁻ groups in the axial position. This does not mean that the free ligand would assume the half-planar structure. But the substituted compound has a lower energy barrier for the deformation from tetrahedral to half-planar structure, a larger negative net charge at the central carbon atom, and an exposed, high-lying $2a_1$ orbital, mainly C p_z in character. The C p_z atomic orbital is occupied by 1.52 electrons and therefore available for electrophilic attack.

The Ligand in the Organometallic Complex

What is the nature of the frontier orbitals of the $[\text{CH}_2(\text{BH}_3)_2]^{2-}$ ligand prepared for bonding in **3**? We showed these orbitals in Figure 1; they are shown again, in greater detail, in Figure 2. To distort the ligand from the energy minimum structure to a B-C-B angle of 150° and H-C-H angle of 104° costs 0.54 eV. The levels $2a_1$ and $2b_2$ do not cross during this distortion, and $2b_2$ remains the HOMO.

Of the six high-lying MOs, three ($2b_2$, b_1 , and a_2) are not localized much in the region of space likely to overlap with the $[\text{Cp}_2\text{M}]^{2+}$ fragment—they are to be identified as B-C or C-H bonding orbitals. The other orbitals, however do “point” toward the metal. Notice the C p_z character of the partially planar carbon in $1a_1$ and $2a_1$ and the substantial H(B) 1s contribution especially in $1b_2$.

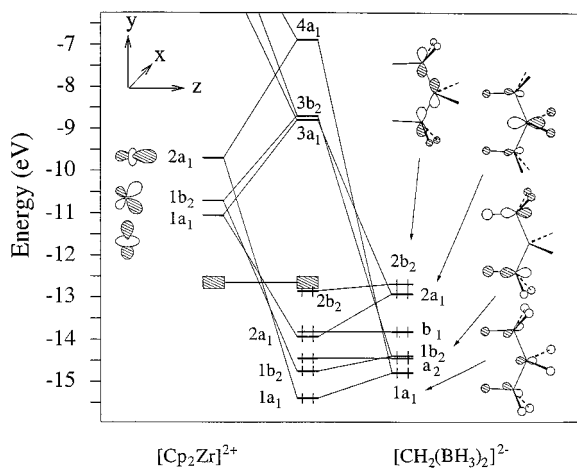


Figure 3. Orbital interaction diagram forming **4**. The Cp's of the $[Cp_2Zr]^{2+}$ fragment in the MOs of $2a_1$, $1b_2$, and $1a_1$ have been omitted for clarity.

The origin of this polarization phenomenon is illuminated by a comparison of the isoelectronic molecules CH_4 and $[BH_4]^-$. Although CH_4 is a poor ligand in organometallic chemistry,²¹ $[BH_4]^-$ complexes are well-known.²² Boron is more electropositive than carbon, and isoelectronic substitution of C by B^- will create changes in the wavefunction and orbital energies. With a change in the electronegativity of a substituent, the Coulomb integral $\langle \Psi_A | H | \Psi_A \rangle = H_{aa}$ varies, decreasing for more electronegative substituents if the geometry is the same, and the overlap integrals are not affected. Any orbitals containing atoms of the more electronegative type are consequently lowered.²³ The t_2 orbitals of tetrahedral CH_4 are in fact 1.1 eV lower in energy than those of $[BH_4]^-$.

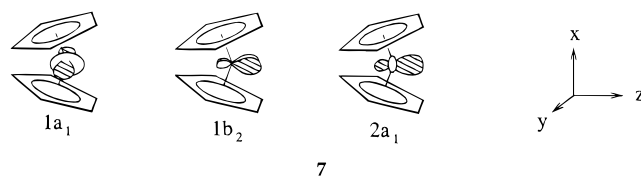
A second consequence of such an electronegativity perturbation is a change in localization of the MOs; the percentage of the H 1s basis functions in the t_2 orbitals of tetrahedral $[BH_4]^-$ is higher (65.2%) than in CH_4 (52.0%). This leads to a higher net charge on the hydrogen atoms of $[BH_4]^-$. We calculate an average net charge of -0.243 per hydrogen atom for $[BH_4]^-$ and $+0.029$ for CH_4 . Roughly speaking, the negative charge in $[BH_4]^-$ is not at the central boron but equally distributed among the hydrogen atoms. Both factors lead to a $B-H^-$ unit capable of better donor coordination through hydrogen to a transition metal fragment.

The Complex

We are ready to construct the bonding in our model of complex **3** with its unusual 5-fold coordinated carbon atom. We show in Figure 3 a portion of the interaction

diagram computed with the EH method illustrating the bonding of $[CH_2(BH_3)_2]^{2-}$ and the bent metallocene unit $[Cp_2Zr]^{2+}$.

The highest occupied MOs of the metallocene moiety (shown in Figure 3 as a shaded block) are mainly localized at the ligand and can be described as π MOs of the Cp ring. Crucial for the resulting stabilization interactions and the bonding in the complex are the acceptor capabilities of the low-lying unfilled $[Cp_2Zr]^{2+}$ MOs $1a_1$, $1b_2$, and $2a_1$, which are localized at the metal center (see left side of Figure 3). These orbitals are familiar, recurring as the frontier orbitals of Cp_2M fragments,²⁴ and they are drawn out schematically in **7**. The $1a_1$ orbital is directed mainly along the y axis and can be described as a d_{yz} orbital, MO $1b_2$ is mainly of d_{xz} character, and $2a_1$ is a hybridized MO pointing along the z axis.



All these orbitals are involved in bonding. The Cp_2M orbitals $2a_1$, $1b_2$, and $1a_1$ interact very efficiently with the ligand orbitals $1a_1$, $1b_2$, and $2a_1$. Important overlaps and resulting contributions to the overlap populations (adding up to 0.736 out of a total inter-fragment overlap population of 0.995) of these interactions are given as follows:

Cp_2M orbital	ligand orbital	overlap	overlap population
$2a_1$	$1a_1$	0.349	0.237
$1b_2$	$1b_2$	0.289	0.238
$1a_1$	$2a_1$	0.239	0.311

The stabilization that results for these MOs is shown in Figure 3. Ligand MO $2b_2$ is almost unaffected by interaction with the MOs of the $[Cp_2Zr]^{2+}$ unit going over into MO $2b_2$ of complex **4**. The same goes for the b_1 and a_2 orbitals. For **4**, ligand MO $2b_2$ is involved in a weak, net repulsive interaction with one low-lying, filled MO of b_2 symmetry of the $[Cp_2Zr]^{2+}$ unit. For **5** and **6**, however, the orbital analogous to $2b_2$ shown in Figure 3 is the HOMO of the complex. It has very small contributions of Zr orbitals. The corresponding MO plots of the four occupied molecular orbitals $2b_2$, $2a_1$, $1b_2$, and $1a_1$ of **4**, computed at the EH level of theory, are shown in Figure 4.

It is clear that in this system the ligand is ideally disposed to bond with the $[Cp_2Zr]^{2+}$ orbitals. Altogether we get bonding Zr–H, Zr–B, and Zr–C interactions.

Figure 5 illustrates the Zr–C, Zr–H, and Zr–B molecular orbital overlap population (MOOP)²⁵ of the MOs of the composite molecule in the valence region. What this graph plots is the contribution of the orbitals at any energy to the total overlap population. Note that the horizontal scale of the MOOP diagrams is arbitrary: the peak heights or integrations of MOOPs for different bond types are not comparable. All three low-

(21) Little is known about the role of alkane complexes, so called " σ complexes" in C–H activation; see e.g.: (a) Arndtsen, B. A.; Bergman, R. G.; Mobley, A.; Peterson, T. H. *Acc. Chem. Res.* **1995**, *28*, 154. (b) Crabtree, R. H. *Angew. Chem.* **1993**, *105*, 828; *Angew. Chem., Int. Ed. Engl.* **1993**, *32*, 789. (c) Brookhart, M.; Green, M. L. H.; Wong, L.-L. *Prog. Inorg. Chem.* **1988**, *36*, 1.

(22) (a) Marks, T. J.; Kolb, J. R.; *Chem. Rev.* **1977**, *77*, 263. (b) Toogood, G. E.; Wallbridge, M. G. H. *Adv. Inorg. Chem. Radiochem.* **1982**, *25*, 267. (c) Barron, A. R.; Scott, J. E.; Wilkinson, G.; Montevalli, M.; Hursthouse, M. B. *Polyhedron* **1986**, *5*, 1833. For a recent theoretical investigation on BH_4 complexes see: (d) Oishi, Y.; Albright, T. A.; Fujimoto, H. *Polyhedron* **1995**, *14*, 2603.

(23) (a) Heilbronner, E.; Bock, H. *Das HMO Modell und seine Anwendung*; VCH: Weinheim, Germany, 1976. (b) Jorgensen, W. L.; Salem, L. *The Organic Chemist's Book of Orbitals*; Academic Press: New York, 1973.

(24) Lauher, J. W.; Hoffmann, R. *J. Am. Chem. Soc.* **1976**, *98*, 1729.

(25) MOOP is a "solid-state-like" plot of the contribution of individual orbitals to the specified overlap population. For the solid-state analogue see: Hoffmann, R. *Solids and Surfaces, A Chemist's View of Bonding in Extended Structures*; VCH: Weinheim, Germany, 1988.

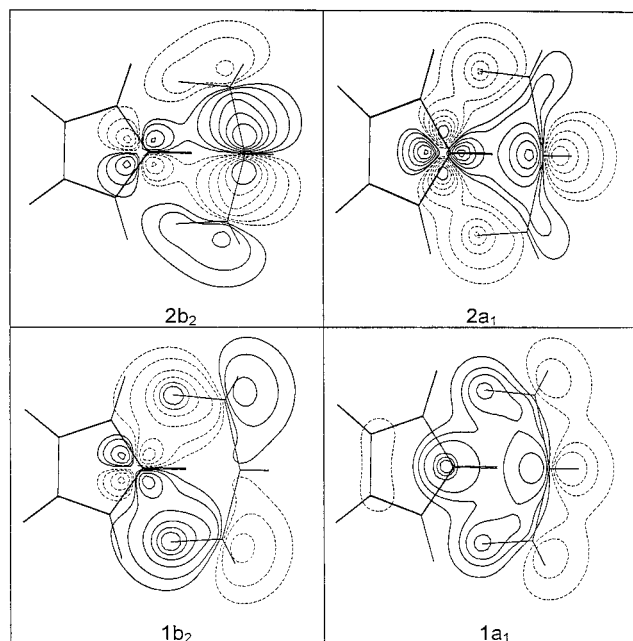


Figure 4. Contour plots of $2b_2$, $2a_1$, $1b_2$, and $1a_1$. The values of the contour lines are ± 0.02 , 0.04 , 0.06 , 0.1 for $1a_1$ and ± 0.02 , 0.04 , 0.08 , 0.12 , 0.16 , 0.20 for the other orbitals. $1a_1$ has 18.95% Zr s character (out of a total Zr contribution of 32.03%).

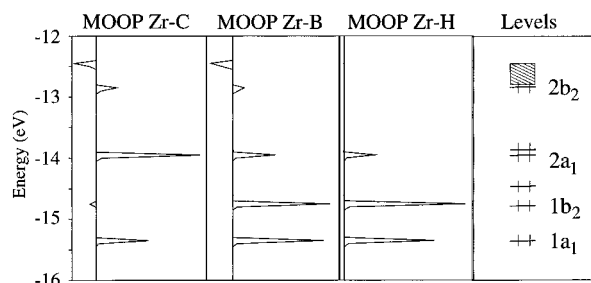


Figure 5. MOOP of Zr–C, Zr–B, and Zr–H in **4**.

lying orbitals ($1a_1$, $1b_2$, $2a_1$) are weakly Zr–B bonding. The MO's $1b_2$ and $1a_1$ are Zr–H bonding in character.

What about the special feature of this molecule, the Zr–C bonding? The Zr–C overlap population results almost entirely from composite molecule MO $2a_1$. Thus, our critical carbon p_z orbital is stabilized mainly by one MO of the zirconocene fragment acting as a σ -acceptor. Most significantly, the atomic orbital occupation of C p_z decreases by 0.23 electrons, whereas the occupations of s, p_x , and p_y remain almost constant (see Table 2). If we calculate a hypothetical $[\text{CH}_2(\text{BH}_3)_2]^{2-}$ ligand interacting with just a proton (a model for an external Lewis acid) at the carbon atom, we obtain a decrease in the population in C p_z of 0.35 electrons, to 0.911 electrons. This type of σ -acceptor stabilization is also found in "ate" complexes with five-coordinate carbon atoms,⁸ where lithium counterions provide the necessary acceptor orbitals.

Table 2 shows important calculated values of overlap populations, atomic orbital occupations, and net charges calculated for the model complexes $\text{Cp}_2\text{Zr}[\text{CH}_2(\text{BH}_3)_2]$, **4**, and for the full structure of **3**. Calculations for the methyl- and fluoride-substituted complexes **5** and **6** are in substantive agreement with the full structure. In the following we will restrict our discussion to the simplest model, $\text{Cp}_2\text{Zr}[\text{CH}_2(\text{BH}_3)_2]$, **4**.

Table 2. Calculated Values of Important Atomic Orbital Occupations, Net Charges, and Overlap Populations of $\text{Cp}_2\text{Zr}[\text{CH}_2(\text{BH}_3)_2]$, **4**, and $\text{Cp}_2\text{Zr}[\text{CH}_2(\text{BH}(\text{C}_6\text{F}_5)_2)_2]$, **3**, from Extended Hückel Calculations

	$\text{Cp}_2\text{Zr}[\text{CH}_2(\text{BH}_3)_2]$, 4 complex	ligand alone	$\text{Cp}_2\text{Zr}[\text{CH}_2(\text{BH}(\text{C}_6\text{F}_5)_2)_2]$, 3 complex ^a
Atomic Orbital Population			
C s	1.286	1.308	1.291
C p_x	0.964	0.968	0.990
C p_y	1.181	1.213	1.201
C p_z	1.037	1.265	1.038
Net Charge			
Zr	0.581		0.528
C	-0.467	-0.754	-0.520
B	0.369	0.113	0.578
H(3,4)	0.049	0.036	0.057
Overlap Population			
Zr–C	0.289		0.273
Zr–B	0.155		0.145
Zr–H(1,2)	0.280		0.292
Zr–H(3,4)	-0.031		-0.029
C–H(3,4)	0.782	0.798	0.780
B–C	0.565	0.636	0.573

^a The geometry suggested by the published X-ray structure determination was used and values averaged where necessary.

As Table 2 indicates, and as we implied above, we calculate a significant overlap population between Zr and all other members of the metallaheterocyclic ring, i.e. for Zr–C, Zr–H(B), and Zr–B as well. The overlap populations, Zr–H(B) = 0.280, Zr–B = 0.155, and H–B = 0.548, are comparable to those in a hypothetical $\text{Cp}_2\text{ZrH}(\eta^2\text{-BH}_4)^{26}$ with a geometry resembling the geometry of the Zr–H–B moiety of our model. The calculated values for this model compound are 0.245 for Zr–H ($d = 1.95$ Å), 0.212 for Zr–B ($d = 2.37$ Å), and 0.592 for B–H ($d = 1.15$ Å).

For Zr–C we calculate a reduced overlap population of 0.289, which is definitely less than what we find for a model of a full Zr–C single bond, 0.540 in $\text{Cp}_2\text{Zr}(\text{CH}_3)_2$ (with a hypothetical bond length Zr–C of 2.42 Å). But the overlap population is near the Zr–C_{inside} overlap population in d^2 $\text{Cp}_2\text{Zr}(\eta^2\text{-C}_2\text{H}_4)(\text{PMe}_3)^{13}$ or d^0 $[\text{Cp}_2\text{Zr}(\eta^2\text{-C}_2\text{H}_4)\text{Me}]^+.²⁷ In these complexes we obtain for Zr–C_{inside} distances of 2.42 Å (and planar ethylene ligands) overlap population values of 0.315 and 0.276, respectively.$

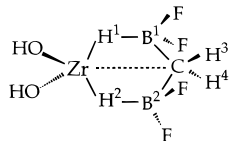
Investigation of the B–C Bond

Our calculations on the extended Hückel level show for each model an interesting decrease of the B–C overlap population for the coordinated ligand. In $\text{Cp}_2\text{Zr}[\text{CH}_2(\text{BH}_3)_2]$, **4**, for example, the B–C overlap population is 0.565 compared to 0.636 in the uncoordinated ligand $[\text{CH}_2(\text{BH}_3)_2]^{2-}$. This decrease is analyzed by a natural bond orbital (NBO) analysis, on a RHF single point calculation on $\text{Cp}_2\text{Zr}[\text{CH}_2(\text{BHMe}_2)_2]$, **5**, and $\text{Cp}_2\text{Zr}[\text{CH}_2(\text{BHF}_2)_2]$, **6**. The canonical MOs of the RHF wave function of **5** and **6** have been transformed into a set of natural bond orbitals (NBOs) according to the

(26) (a) James, B. D.; Nanda, R. K.; Wallbridge, M. G. H. *Inorg. Chem.* **1967**, *6*, 1979. (b) Marks, T. J.; Kennelly, W. J.; Kolb, J. R.; Shimp, L. A. *Inorg. Chem.* **1972**, *11*, 2540. (c) Marks, T. J.; Kolb, J. R. *J. Am. Chem. Soc.* **1975**, *97*, 3387.

(27) (a) Marks, T. J. *Acc. Chem. Res.* **1992**, *25*, 57. (b) Jordan, R. F. *Adv. Organomet. Chem.* **1991**, *32*, 325. (c) Wu, Z.; Jordan, R. F. *J. Am. Chem. Soc.* **1995**, *117*, 5867.

Table 3. Wiberg Bond Indices (wb_i) in the NAO Basis for 6'' and Energy Contributions ΔE_{ij} (kcal/mol) Coming from Interactions between Donor Natural Bond Orbitals (NBOs) with the Occupation Numbers (n_i) and Low Occupied Acceptor Orbitals



σ-bond	wb _i		n _i		ΔE _{ij} complex
	complex	ligand	complex	ligand	
Zr–C	0.316				
Zr–H(1)	0.297				
Zr–H(2)	0.297				
Zr–B(1)	0.130				
Zr–B(2)	0.130				
Zr–H(3)	0.013				
Zr–H(4)	0.009				
B(1)–C	0.741	0.763	1.873	1.980	33.0
B(2)–C	0.741	0.763	1.873	1.980	33.0
H(1)–B(1)	0.597	0.879	1.755	1.993	106.9
H(2)–B(2)	0.597	0.879	1.755	1.993	106.9
C–H(3)	0.856	0.958	1.952	1.982	
C–H(4)	0.856	0.940	1.952	1.971	

Weinhold NBO localization procedure.²⁸ We discuss in the following model 6''; the analysis for 5 or 6 is in substantial agreement with the data shown below.

In Table 3 we have compared the Wiberg bond indices²⁹ of the natural atomic orbital (NAO) as well as the occupation numbers (n_i) of 6'' with those of the [CH₂(BHF₂)₂]²⁻ ligand. The Wiberg bond indices (Table 3) indicate a significant interaction between Zr and all other members of the metallaheterocyclic ring. These values confirm the qualitative conclusions of the EH calculation.

We searched in our NBO analysis for two-electron three-center bonds in the metallaheterocyclic ring. According to our analysis only the Zr, H, and B atoms are mutually engaged in two-electron three-center bonds. The data of Table 3 reveal that both H–B σ bonds (n_i = 1.755) of 6'' are strongly delocalized, and the two B–C σ bonds (n_i = 1.873) are delocalized to a smaller extent, compared to the free ligand (Table 3). According to second-order perturbation theory, a stabilization energy ΔE_{ij}³⁰ associated with high (donor) NBO_(i) and low (acceptor) NBO_(j) is expressed as

$$\Delta E = n_i(F_{ij}^2/\epsilon_j - \epsilon_i) \quad (1)$$

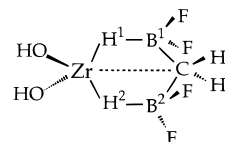
where n_i is the donor orbital occupancy, ε_i and ε_j are diagonal elements, and F_{ij} is the off-diagonal element of the NBO Fock matrix. The substantial ΔE_{ij} value of 106.9 kcal/mol can be assigned to the donor–acceptor interaction between each H–B σ bond with a relatively pure d-orbital acceptor NBO, similar to the 2a₁ metal orbital shown in the left part in Figure 3 (see Table 3). Another smaller donor–acceptor interaction (ΔE_{ij} = 33.0) is between each B–C σ-bond and a d orbital comparable with the 1b₂ level in Figure 3.

(28) (a) Foster, J. P.; Weinhold, F. *J. Am. Chem. Soc.* **1980**, *102*, 7211. (b) Reed, A. E.; Weinstock, R. B.; Weinhold, F. *J. Chem Phys.* **1985**, *83*, 735.

(29) Wiberg, K. *Tetrahedron* **1968**, *24*, 1083.

(30) Reed, A. E.; Curtis, L. A.; Weinhold, F. *Chem. Rev.* **1988**, *88*, 899.

Table 4. Comparison between Experimental (3) and Calculated Bond Lengths and Bond Angles for 6''



	6''		3 exptl
	MP2	DFT	
Distances (Å)			
Zr–C	2.457	2.448	2.419
Zr–B(1)	2.623	2.615	2.614
Zr–B(2)	2.623	2.615	2.650
Zr–H(1)	1.940	1.912	1.978
Zr–H(2)	1.940	1.912	1.941
C–B(1)	1.703	1.673	1.697
C–B(2)	1.703	1.673	1.693
C–H(3)	1.105	1.099	0.934
C–H(4)	1.105	1.099	0.925
Angles (deg)			
B(1)–C–B(2)	151.5	152.4	149.3
B(1)–C–Zr	75.8	76.2	76.6
H(1)–Zr–H(2)	138.2	137.2	126.0
Zr–H(1)–B(1)	104.0	104.8	112.0
Zr–C–H(3)	124.3	125.0	107.0
Zr–C–H(4)	124.3	125.0	149.0

Looking for a Potential Agostic Interaction

In their original paper, Piers et al.¹² attributed the skewing they found for the methylene unit of 3 to a potential agostic interaction between methylene hydrogen atoms and the metal center. Neither for 3 nor for our model 4 did we calculate a bonding overlap population for Zr–H(3) on the extended Hückel level. In both cases we got a slightly negative overlap population of –0.031 and –0.040, respectively (see Table 2).

In order to investigate the possible existence of an agostic Zr–H interaction at a higher level of calculation, we predisposed 5 and 6 for such an interaction by taking the values for the Zr–C–H(3) = 107.0° and Zr–C–H(4) = 149.3° angles from the X-ray data of 3. In neither case we could find a donor–acceptor interaction for the C–H(3) σ bond. We think there is no reason to assign an agostic interaction to this bond. One further attempt to find such an interaction, described in the next section, also failed.

Geometry Optimizations of 5', 6', and 6''

We have optimized the geometry of compounds 5', 6', and 6'' by applying the RHF, RMP2, and DFT methods. The values obtained for (HO)₂Zr[CH₂(BHF₂)₂], 6'', are shown in Table 4.

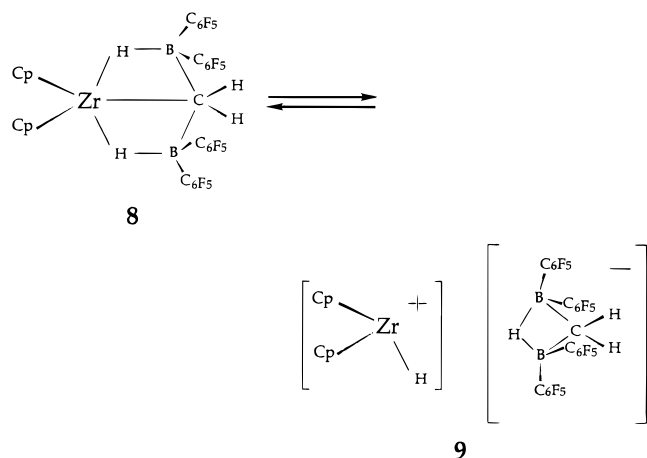
The calculated geometrical parameters of 6'' (L = OH) are in good agreement with the X-ray data obtained from 3. Those of 6' (not shown in Table 4) are not that different. The values for the 5' model, not reported here, differ, in part significantly. Especially the calculated value for the B–C distance was too long. Thus the fluoride ligand seems to be a better substituent model than the methyl group for the C₆F₅ unit, since the σ-acceptor and π-donor interactions of the F ligand appear to be comparable with those of the C₆F₅ ligand.

The positions obtained for the hydrogen atoms in the metallaheterocycle are different from those of the crystal structure. We have also performed RMP2 geometry

optimization without symmetry constraints for model **6'** and **6''**. However, we obtained nearly the same geometrical parameters (within 0.01 Å for all distances, within 0.3° for all angles). A skewing of the methylene group, in the sense encountered by the crystal structure determination, was *not* found. We think therefore that this skewing, if real, should be attributed to steric or packing effects. Further evidence for the hydrogen positions could be obtained by neutron diffraction.

Implications for the Catalytic Activity of **3**

Piers et al. suggested in their paper¹² a possible equilibrium between complex **3** and its ionic fragmentation products, as indicated in **8** → **9**. Studies of similar complexes by Marks et al.³¹ point to such species as catalysts for ethylene polymerization.



As a consequence of such an equilibrium, a reduction in the activity of the catalyst might be expected. We have estimated the difference in energy between **6''** and the appropriate ionic fragments **9''**, $[(\text{HO})_2\text{ZrH}]^+[\text{CH}_2(\text{BF}_2)_2(\mu\text{-H})]^-$, at the RMP2 level. According to our calculations the fragments **9''** are approximately 143 kcal/mol less stable than **6''**. In a similar calculation, we obtain for **6'** and **9'**, $[\text{Cl}_2\text{ZrH}]^+[\text{CH}_2(\text{BF}_2)_2(\mu\text{-H})]^-$, an energy difference of 164 kcal/mol. We considered neither solvation effects of the ions **9''** in our computations nor attractive electrostatic interactions between them. Thus the value 143 kcal/mol is an upper limit. Furthermore we have computed the difference in energy between **6''** and the appropriate neutral molecules **10''**, $[(\text{HO})_2\text{ZrH}_2]$, and **11'**, $[\text{CH}_2(\text{BF}_2)_2]$, at the RMP2 level. The optimized structures of the ionic fragments and neutral molecules are shown in Figure 6.

The calculated bonding parameters of the anion-part **9''** are in good agreement with the X-ray structure of $[\text{tBuCH}_2\text{CH}(\text{B}\{\text{C}_6\text{F}_5\}_2)_2\text{H}]$ determined by Marks et al.³¹ The carbon atom is tetrahedrally coordinated in the neutral fragment **11'**, whereas the carbon atom in complex **3** is half-planar. Our computations predict that **6''** is only 14 kcal/mol more stable than the neutral molecules **10''** and **11'** (for **6'** and **10'** and **11'** we obtain 5 kcal/mol). As a consequence of our computations we suggest rather a possible equilibrium between complex **3** and its neutral fragmentation products, indicated as follows:

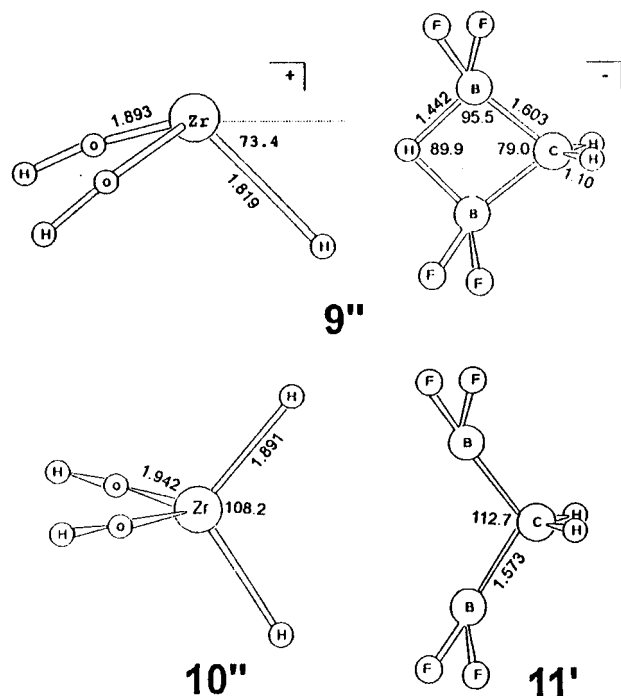
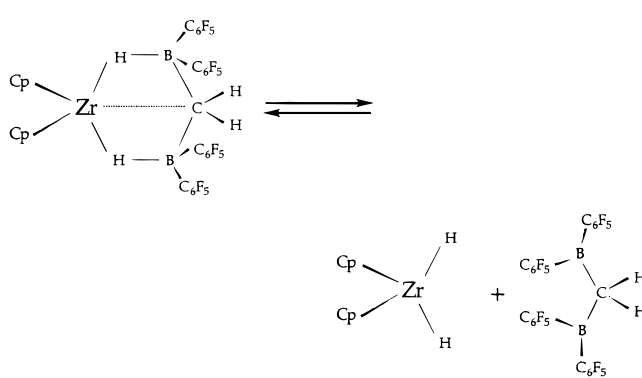


Figure 6. Optimized structure of the ionic fragments **9''** and the neutral molecules **10''** and **11'**.



Conclusions

The methylene carbon atom of **3** with its exceptional distorted "trigonal-bipyramidal" or "part-planar" geometry is stabilized by (i) two good σ -donor groups in axial positions and (ii) a bond to an external σ -acceptor orbital of the metallocene unit. We certainly find for this methylene carbon atom bonding overlap populations to five atoms in its coordination sphere; in the "equatorial" plane of the five-coordinate carbon two bonds to hydrogen atoms and a Zr-C bond are formed. The bond strength of the latter is comparable to the Zr-C_{inside} bond in $\text{Cp}_2\text{Zr}(\eta^2\text{-C}_2\text{H}_4)(\text{PMe}_3)$ and $[\text{Cp}_2\text{Zr}(\eta^2\text{-C}_2\text{H}_4)\text{Me}]^+$. In the axial plane the carbon binds to two boron atoms, with a bond weaker than that in an analogous tetrahedral geometry. The known complexes containing trigonal-bipyramidal pentacoordinated carbon atoms stabilize this geometry in similar ways, i.e. by σ -donor and/or π -acceptor ligands in the axial plane and by coordination to an external σ -acceptor in the equatorial plane.

From another viewpoint, the essential feature of the binding of $[\text{Cp}_2\text{Zr}]^{2+}$ to the $[\text{CH}_2(\text{HBR}_2)_2]^{2-}$ unit is that all five chelating atoms, H(B), B, C, B, and H(B), get involved in bonding, optimally utilizing the bonding capabilities of the two a_1 and the b_2 orbitals of the Cp_2M

(31) Jia, L.; Yang, X.; Stern, C.; Marks, T. J. *Organometallics* **1994**, *13*, 3755.

Table 5. EH Parameters Used in the Calculation

	H_{ii}	ζ_1	c_1	ζ_2	c_2
Zr 5s	-9.87	1.817			
Zr 5p	-6.76	1.776			
Zr 4d	-11.18	3.835	0.621	1.505	0.5769
C 2s	-21.40	1.625			
C 2p	-11.40	1.625			
F 2s	-40.00	2.425			
F 2p	-18.10	2.425			
B 2s	-15.20	1.300			
B 2p	-8.50	1.300			
H 1s	-13.60	1.300			

Table 6. Important Bond Distances and Bond Angles of Our Model

distances (Å)		angles (deg)	
Zr-C	2.42	H-Zr-H	128.6
Zr-B	2.57	Zr-H-B	111.2
Zr-H(1,2)	1.92	H-B-C(H ₂)	109.5
B-C(H ₂)	1.70	B-C-B	150.0
B-CH ₃	1.65	H-C-H	104.0
C-H	1.10		
C-F	1.40		

fragment. The resulting six-membered ring, stabilized by the interaction of Zr to all other members of that metallaheterocycle, enables the methylene carbon atom to enlarge its B-C-B angle.

Acknowledgment. Thanks are due to Greg Landrum for help with using his program and to the reviewers of our paper for useful suggestions. U.R. thanks the Deutsche Forschungsgemeinschaft (DFG) for a postdoctoral fellowship which made his stay at Cornell University possible. Our work at Cornell was supported by Research Grant CHE 94-08455. The work at Heidelberg was supported by the Volkswagenstiftung, the Deutsche Forschungsgemeinschaft, and the Fonds der Chemischen Industrie.

Appendix: Details of the EH Calculations

The extended Hückel calculations³² were done using Greg Landrum's YAeHMOP program.³³ The parameters used were taken from previous work^{32a,34} and are listed in Table 5. Table 6 shows some important distances and angles used in our model.

OM960099B

(32) (a) Hoffmann, R. *J. Chem. Phys.* **1963**, *39*, 1397. (b) Hoffmann, R.; Lipscomb, W. N. *J. Chem. Phys.* **1962**, *36*, 2179. (c) **1962**, *36*, 3489. (d) **1962**, *37*, 2872.

(33) Landrum, G. *YAeHMOP*—Yet Another extended Hückel Molecular Orbital Package, version 1.1, Ithaca, NY, 1995. This package is available on the WWW at the following address: <http://overlap.chem.cornell.edu:8080/yaehmop.html>.

(34) (a) Tatsumi, K.; Nakamura, A.; Hofmann, P.; Stauffert, P.; Hoffmann, R. *J. Am. Chem. Soc.* **1985**, *107*, 4440. (b) Anderson, A. B.; Hoffmann, R. *J. Chem. Phys.* **1974**, *60*, 4271.